Strain relaxation mechanisms and local structural changes in Si$_{1-x}$Ge$_x$ alloys

Ming Yu,[1] C. S. Jayanthi,[1] David A. Drabold,[2] and S. Y. Wu[1]

[1]*Department of Physics, University of Louisville, Louisville, Kentucky 40292*

[2]*Department of Physics and Astronomy, and Condensed Matter and Surface Sciences Program, Ohio University, Athens, Ohio 45701-2979*

In this work, we address issues pertinent to the understanding of the structural and electronic properties of Si$_{1-x}$Ge$_x$ alloys, namely, (i) how does the lattice constant mismatch between bulk Si and bulk Ge manifest itself in the alloy system? and (ii) what are the relevant strain release mechanisms? To provide answers to these questions, we have carried out an in-depth study of the changes in the local geometric and electronic structures arising from the strain relaxation in Si$_{1-x}$Ge$_x$ alloys. We first compute the optimized lattice constant for different compositions (x) by fully relaxing the system and by minimizing the total energy with respect to the lattice constant at each composition, using an *ab initio* molecular dynamics scheme. The optimized lattice constant, while exhibiting a general trend of linear dependence on the composition (Vegard's law), shows a negative deviation from Vegard's law in the vicinity of $x=0.5$. We delineate the mechanisms responsible for each one of the above features. We show that the radial-strain relaxation through bond stretching is responsible for the overall trend of linear dependence of the lattice constant on the composition. On the other hand, the negative deviation from Vegard's law is shown to arise from the angular-strain relaxation. More specifically, the combined effect of the local bond-angle deviations from the tetrahedral angle and the magnitudes of the corresponding peaks for the partial-angle distribution function determines the negative deviation from Vegard's law. The electronic origin of the changes in the local geometric structure due to strain relaxation is also presented in this work. In particular, the correlation between the bond charges and the bond-lengths for Si-Si, Ge-Ge, and Si-Ge pairs in Si$_{1-x}$Ge$_x$ alloys for different compositions is explicitly shown. Our calculation of the average coordination number as a function of composition indicates a random occupation of Si and Ge on the lattice sites, suggesting that Si and Ge atoms are fully miscible in the alloy system.

I. INTRODUCTION

It is well known that the 4% difference in the experimentally observed lattice constants between bulk Si and bulk Ge gives rise to a significant strain in the growth of Si$_{1-x}$Ge$_x$ alloys, and the relaxation of the strain causes changes both in the local geometric structure and in the electronic structure of Si$_{1-x}$Ge$_x$ alloys as compared to those of pure Si and Ge. In order to understand the mechanism of the strain relaxation, extensive experimental[1-11] and theoretical[12-19] efforts have been devoted to the study of the interplay between the relaxation of the strain and the changes in local geometric and electronic structures. Most experiments[3,9-11] found that the lattice constant as a function of the composition does not follow an exact linear relation such as the one given by the Vegard's model[20] but has a negative deviation from the Vegard's law. The bond lengths, on the other hand, show a weak composition dependence.[1,2,4-8] But they do not obey the Pauling model[21] in which the bond length between a pair of atoms is independent of composition, and the steric strain in the alloys is accommodated by bond-angle changes.

A number of theoretical studies have been devoted to the local structural analysis of Si$_{1-x}$Ge$_x$ alloys at an empirical or at the semi-empirical level. Weidmann and Newman[13] by minimizing a model strain energy function found that the bond lengths between Si-Si, Si-Ge, and Ge-Ge pairs as a function of composition are straight lines and parallel to each other. Similar result were also obtained by Ichimura *et al.*[14] and Gironcoli *et al.*[15] Alternatively, Thorpe and

co-workers[17,18] proposed a simplified model on the basis of macroscopic elastic properties. The composition dependence of the bond lengths is described via a topological rigidity parameter a^{**} which leads to the Vegard limit when $a^{**}=0$ and to the Pauling limit when $a^{**}=1$. According to their model, a^{**} should be 0.707 for SiGe alloys, and a plot of the Si-Si, Si-Ge, and Ge-Ge bond lengths versus composition should consist of three equally spaced parallel lines having a slope that is directly related to the value of a^{**}.

These previous theoretical studies, while attempting to provide the insight into how the local structural properties accommodate the relaxation of the strain, failed to predict the weak dependence of the bond lengths of Si-Si, Si-Ge, and Ge-Ge on the composition. They also did not reproduce the negative deviation of the lattice constant from the Vegard's law. For example, the result given in Ref. 18 predicted a linear dependence on the composition for the lattice constant while the result by a Monte Carlo simulation[15] yielded a positive deviation from Vegard's law. Another Monte Carlo study using a statistical-mechanical model[19] also obtained an overall linear dependence of the lattice parameter on the composition, but with a hint of negative deviation from Vegard's law in the vicinity of $x \simeq 0.5$. An effort to resolve these issues had been carried out by Shen *et al.*,[22] using a semi-empirical tight-binding method in the dilute limit. The model described reasonably well the behavior of the lattice constant and the properties of bond lengths in this dilute limit. However, no attempt was made to correlate the model of strain relaxation and the local properties in this study.

Very recently, a more accurate experimental measurement of the local structure at all compositions has been reported by Aubry *et al.*[9] They analyzed the K-edge x-ray absorption fine structure (XAFS) spectra of Si and Ge in strained and relaxed $Si_{1-x}Ge_x$ alloys. They found that the Si-Si, Si-Ge, and Ge-Ge first-shell distances show a weak dependence on the composition. The slopes of the linear fits to the bond lengths as a function of the composition are demonstrably different from each other.[9] This result is different from the previous theoretical predictions. They also confirmed from the composition dependence of the coordination numbers that the Si and Ge atoms are likely to be randomly occupying the sites and are fully miscible at all compositions.

An accurate theoretical determination of equilibrium configurations of $Si_{1-x}Ge_x$ alloys with no parametric input is highly desirable. This is because such a determination can help to clarify issues related to the whole spectrum of available experimental observations. Furthermore, it can shed light on the interplay between the effects of strain relaxation and local properties of the alloys. In this work, we have used the *ab initio* molecular dynamics scheme, as developed by Sankey and co-workers,[23] to carry out the energy minimization for the determination of the equilibrium structures of $Si_{1-x}Ge_x$ alloys at various compositions. A brief outline of this method is given in Sec. II. We then conducted a local analysis of the structural (Sec. III) as well as electronic properties (Sec. IV) of the relaxed configurations. Corresponding to each composition, we have computed the optimized lattice constant, bond lengths, coordination numbers, and pair-correlation functions (radial and angular). The results of these calculations are used to identify the mechanisms for strain release and to explain succinctly the origin of Vegard's law as well as the deviation from this law for x in the vicinity of 0.5. The conclusions drawn from this work are given in Sec. V.

II. METHOD

The *ab initio* molecular dynamics scheme employed in the present work is based on the density-functional theory (DFT) in the local-density approximation (LDA), as developed by Sankey and co-workers,[23] where a local basis set is used to construct the Kohn-Sham orbitals. These basis functions are slightly excited pseudoatomic orbitals (PAO). The Kohn-Sham orbitals are calculated self-consistently using the Hamann-Schlüter-Chiang pseudopotentials[24] and the Ceperley-Alder form of the exchange-correlation potential, as parametrized by Perdew and Zunger.[25] The use of PAO's as basis set is extremely convenient in studies which require extracting information about local structural and electronic properties of complex systems such as $Si_{1-x}Ge_x$ alloys. For complex systems with reduced symmetry, the computational performance of this method as far as the CPU time is concerned is better than other *ab initio* methods based on plane-wave basis sets.

In our simulation, sp^3-type PAOs were used with confinement radii of 5.0 a_B and 5.2 a_B for Si and Ge atoms, respectively. The initial network chosen has a tetrahedral symmetry with 216 atoms in a cubic unit cell. For a given

volume and composition, the network was fully relaxed by the dynamical quenching method using the quantum-molecular dynamics scheme cited above. The equilibrium configuration was considered to have been reached when the force on each atom is less than 1×10^{-2} eV/Å . We evaluated the total energy convergence by using both 1 and 8 special k points in the BZ and found that the result of using 8 k points only improves the accuracy by 1×10^{-2} eV. Therefore, we adopted the Γ point calculation in the ensuing simulations. The volume optimization was carried out by minimizing the total energy with respect to the lattice constant for a given composition. We then conducted a local analysis of the structural and electronic properties corresponding to each composition.

III. LOCAL ANALYSIS OF STRUCTURAL PROPERTIES

In a recent experimental study on local structural properties of $Si_{1-x}Ge_x$ alloys, Aubry *et al.* concluded from the composition dependence of the coordination numbers that Si and Ge atoms are likely to be randomly occupying the sites and are fully miscible at all compositions. In order to provide a theoretical confirmation of the conclusion drawn by Aubry *et al.*, we carried out studies on two types of alloy models: (i) a nonrandom alloy and (ii) a random alloy. In the nonrandom alloy model, Si and Ge atoms are distributed at the sites of the supercell following a rule for a given concentration. The sites in the supercell can be labeled sequentially in a certain order from site 1 through N where N is the total number of atoms in the supercell. The assignments of Si and Ge atoms at the sites are carried out in a pattern according to their concentrations. For example, in the case of $Si_{0.75}Ge_{0.25}$, the assignment of Si and Ge atoms at a given site proceeds following the rule of one Ge atom after every three Si atoms. Thus the nonrandom alloy consists of arbitrary configurations but with a correlation among the distribution of atomic species in the system. The purpose here is to determine how the composition dependence of the coordination numbers for a configuration with a correlation among the distribution of atomic species compares with the experimental observation. In the *random* alloy model, the Si and Ge atoms are (completely) randomly distributed. We found that the total energy difference between these two cases is quite small (within the error bar), but the coordination numbers as a function of the composition are quite different as shown in Fig. 1. It is found that the *nonrandom* alloy (open symbols) can not explain the experimental result[9] (see the inset), but the *random* alloy (solid symbols) mimics the experimental result very well.

The two kinds of average coordination numbers that are relevant to alloys are defined as $N_{average} = \Sigma_i^N n_i / N$ and $N_{\alpha\beta} = \Sigma_{i_\alpha}^{N_\alpha(\beta)} n_{i_\alpha}(\beta) / N_\alpha(\beta)$, respectively, where $N_{average}$ is the coordination number that counts all atom types as neighbors, whereas $N_{\alpha\beta}$ gives the average number of β-type neighbors for the α-type atom within a cutoff R_{cut} with N being the total number of atoms, n_i the number of neighbors of the ith atom, and $N_\alpha(\beta)$ the total number of the α-type atom having β-type atoms as its neighbors. It is clear that $N_{average} = 4$ in the four-fold bonding structure such as tetrahedral symmetry
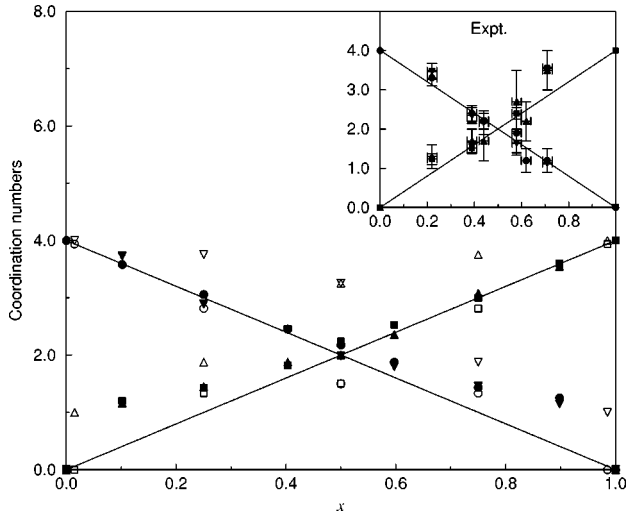
FIG. 1. The calculated coordination numbers as a function of the composition x where the circles denote N_{SiSi}, the up-triangles N_{SiGe}, the down-triangles N_{GeSi}, and the squares N_{GeGe}. The solid symbols correspond to the *random* alloy model and the open ones correspond to the *nonrandom* alloy model. The inset shows the coordination numbers obtained from XAFS results as a function of composition (Ref. 9). The lines indicate the expected coordination numbers on the basis of random site occupancy.
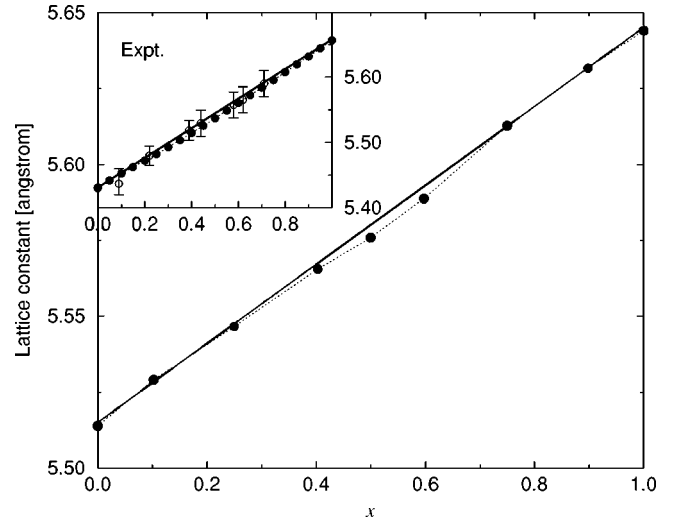

FIG. 2. Optimized lattice constant as a function of the composition x (solid circles). The solid line is the Vegard model prediction. The inset is the experimental measurements where solid circles are from Ref. 10 and open circles (including error bars) are from Ref. 9.

systems, and $N_{\alpha\beta}=1$ when there is only one α (β) atom in the β (α) atom system. If α and β atoms are randomly distributed, there must be no significant difference among $N_{\alpha\alpha}$, $N_{\beta\beta}$, $N_{\beta\alpha}$, and $N_{\alpha\beta}$ at $x=0.5$, and the composition dependence of the coordination numbers must follow the linear dependence outlined by the two straight lines shown in Fig. 1. The coordination numbers of the *random* alloy model clearly show such a behavior as can be seen in Fig. 1 and our results are consistent with the recent experimental measurements.[9] On the other hand, the composition dependence shown by the nonrandom alloy model with a correlation among the distribution of atomic species is quite different from the experimental result. Thus, our results support the notion that Si and Ge atoms randomly occupy the sites and are fully miscible in $Si_{1-x}Ge_x$ alloys because of their similar chemical properties. We therefore concentrated on the *random* alloy model hereafter in our local structural analysis and in the comparison with the experimental results.

We examined the global and local structural properties of $Si_{1-x}Ge_x$ alloys at various compositions ($x = 0$, 0.10, 0.25, 0.40, 0.5, 0.60, 0.75, 0.90, and 1.0). Figure 2 presents the optimized lattice constant versus the composition obtained from the total energy minimization. We found that the lattice constant (solid circle) monotonously increases from 5.513 Å at $x=0$ (corresponding to pure Si) to 5.645 Å at $x=1$ (corresponding to pure Ge) with increasing x. It exhibits a negative deviation from the linear Vegard's law (dashed line). The deviation appears from $x \approx 0.25$, shows the largest deviation around $x=0.5$, and then gradually disappears beyond $x=0.75$, in good agreement with experimental results[9,10] (see the inset). It should be noted that, while the experimental value of the mismatch between bulk Si and bulk Ge is about 4%, our

optimization yields a mismatch of only about 2.4%. Therefore, we present the experimental data of Ref. 9 in the inset rather than in the same figure. Our goal is to compare the trend and the general pattern of the structural changes as a function of concentration so as to deduce an understanding of the strain relaxation mechanisms in $Si_{1-x}Ge_x$ alloys.

The average bond length between a pair of atoms of types α and β, $b_{\alpha\beta}$, is defined as $b_{\alpha\beta}=\Sigma_{i_\alpha}^{N_\alpha}\Sigma_{j_\beta}^{R_{\text{cut}}}d_{i_\alpha,j_\beta}/\Sigma_{i_\alpha}^{N_\alpha}n_{i_\alpha}(\beta)$, where $\alpha(\beta)$ denotes the type of atom, N_α is the total number of α-type atom in the supercell, d_{i_α,j_β} the distance between the α-type atom at the ith site and the β-type atom at the jth site, and $n_{i_\alpha}(\beta)$ the number of neighboring β-type atoms around the α-type atom at the ith site within the cutoff radius of R_{cut}. We took R_{cut} to be 2.7 Å in our analysis which is between the first and the second peaks of the radial-pair distribution function of the relaxed alloy configurations. We examined the choice of R_{cut} in the region of 2.6–3.2 Å and found that the value does not have much influence on the results because the first and the second peaks are well separated by about 1 Å.

Figure 3 illustrates the calculated average bond-lengths of Si-Si, Si-Ge, and Ge-Ge pairs versus the composition x. The experimental data[9] are presented in the inset. Notice that the largest error bar for Si-Si bond length in $Si_{1-x}Ge_x$ alloys occurs at $x \sim 0.75$ while that for Ge-Ge bond length at $x \sim 0.25$.[9] These features had been attributed to the distortions associated with possible compound formation at these concentrations.[9] Turning now to the theoretical result, it can be seen that the variation of both sets of bond lengths (Si-Si and Ge-Ge) with respect to x follows the same general pattern. Overall, the bond lengths are rather insensitive to the composition. For the Si-Si pairs, the increase in their average bond-length is concentrated in the Ge-rich region while for the Ge-Ge pairs, the decrease in their average bond length is
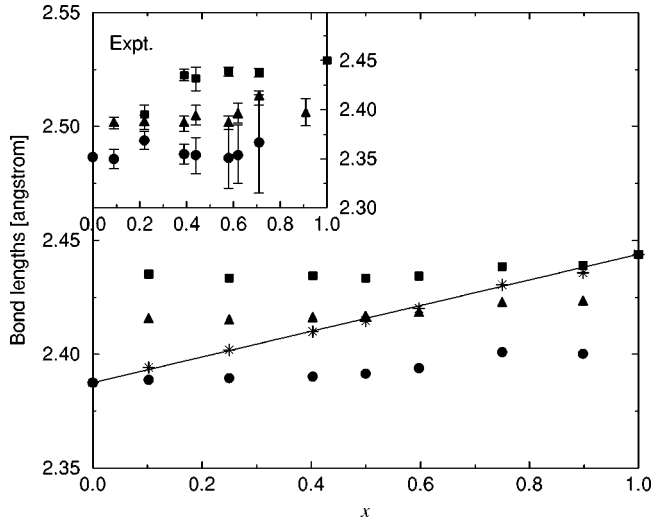
FIG. 3. Calculated average bond lengths as a function of the composition x, where the circles denote b_{SiSi}, the up-triangles b_{SiGe}, and the squares b_{GeGe}. The stars represent the overall average bond lengths calculated by taking into account all three types of bonds without distinguishing any particular bonding pair. A solid line is drawn through these points to provide a guidance to the eye. The inset is the experimental result for the first-shell bond lengths at different compositions (see Fig. 8 in Ref. 9). Notice that the largest error bar for Si-Si bond length in $Si_{1-x}Ge_x$ alloys occurs at $x \sim 0.75$ while that for Ge-Ge bond length at $x \sim 0.25$ (Ref. 9). These features had been attributed to the distortions associated with possible compound formation at these concentrations (Ref. 9).

mostly in the Si-rich region. The Si-Ge pairs appear to form at a distance close to the mean value of the average bond-lengths of Si-Si and Ge-Ge pairs for a given composition. The weak dependence of the average bond lengths of Si-Si and Ge-Ge pairs on the composition indicate that the Si-Si and Ge-Ge pairs prefer to maintain their respective bond length even in the alloying situation. The preference of the Si-Ge pairs to form at distances close to the mean value of the average bond lengths of Si-Si and Ge-Ge pairs is an indication that the mismatch between lattice constants of bulk Si and bulk Ge is accommodated by the formation of the Si-Ge bond. It should be noted that the bond lengths vs the composition curves for Si-Si, Si-Ge, and Ge-Ge bonds obtained in the present calculation do not correspond to equally spaced parallel lines as obtained by previous calculations.[13–15,17,18] They are, however, consistent with the experimental result (see the inset of Fig. 3) as discussed above. It should also be noted that the calculated average bond-length of Si-Si pairs for bulk Si is 2.39 Å, somewhat longer than the experimental value of 2.35 Å while the calculated average bond-length of Ge-Ge pairs for bulk Ge is 2.44 Å, somewhat shorter than the experimental value of 2.45 Å.[11] Thus the spread of the variation of the calculated average bond-lengths versus the composition is narrower than that of the corresponding experimentally observed bond lengths.

We next analyze how the local structure changes due to the strain relaxation. The radial-strain relaxation can be analyzed from the radial-pair distribution function $g_{\alpha\beta}(r)$ for an
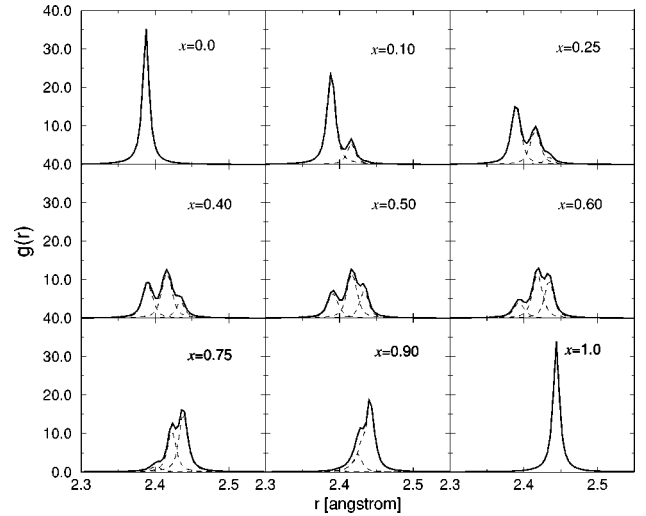

FIG. 4. The total $g(r)$ (solid curves) and partial $g_{\alpha\beta}(r)$ (dashed curves) radial-pair distribution function at compositions of $x = 0.0$, 0.10, 0.25, 0.40, 0.5, 0.60, 0.75, 0.90, and 1.0. Note that the left dashed curves correspond to $g_{SiSi}(r)$, the middle to $g_{SiGe}(r)$, and the right to $g_{GeGe}(r)$, respectively.

α-type atom at the origin and a β-type atom at a distance r away. As shown in Fig. 4, the total radial-pair distribution function $g(r)$ (solid curve) in the region of the first-shell distance consists of three subpeaks: the Si-Si peak on the left side, the Si-Ge in the middle, and the Ge-Ge on the right side (note that these subpeaks can be clearly distinguished at $x = 0.4$, 0.5, and 0.6). Such peak positions shift less than 0.5% from $x = 0.0$ to $x = 1.0$, indicating that during the strain relaxation all the pairs of Si-Si, Si-Ge, and Ge-Ge prefer to be as close to their equilibrium distances as possible. It can also be seen that the 2% shift of the peak position of the average first-shell distance is attributed to the change of the ratio among the Si-Si, Si-Ge, and Ge-Ge pairs in the mixture. This explains the monotonous increase of the lattice constant with increasing Ge composition. Furthermore, the average overall bond length of all three types of bonds has been plotted versus the composition in Fig. 3. It shows a linear dependence on the composition. Hence the strain release through the radial stretching is apparently responsible for the overall trend of linear dependence of the lattice constant on x.

The question is then how does the lattice constant versus x curve exhibit a negative deviation from Vegard's law? Specifically, how does the mismatch between the lattice constants of bulk Si and bulk Ge manifest itself when Si-Si and Ge-Ge pairs prefer to maintain their respective lengths? To answer this question, we examined the bond-angle strain relaxation from the bond-angle distribution function $g(\theta)$. It is seen from Fig. 5 that the peak of the bond-angle distribution is sharp at pure limits and broad at or close to the maximum mixing case ($x = 0.5$). This is an indication that there are large bond-angle distortion where the strain is largest. To understand in more detail how the angular strain affects the local structure, we plotted the 6 partial bond-angle distribution functions $g_{\alpha\beta\gamma}(\theta)$ at $x = 0.25$, 0.5, and 0.75, respectively as shown in Fig. 6. Here $g_{\alpha\beta\gamma}(\theta)$ gives the angular distribution for the angle θ between two bonds $\beta\alpha$ and $\beta\gamma$.
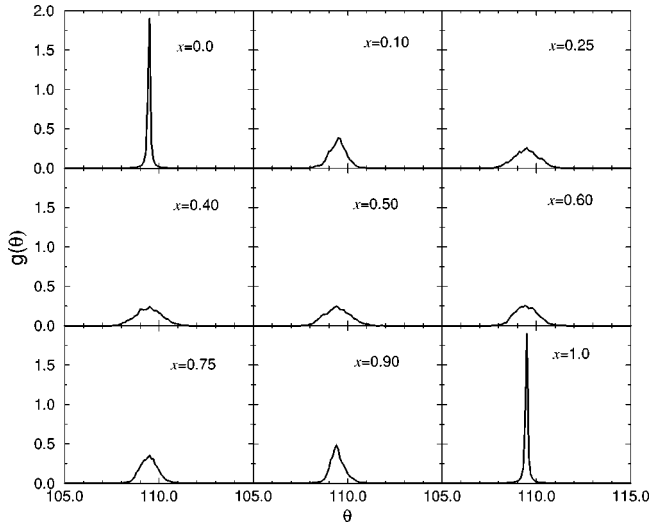
FIG. 5. The total bond-angle distribution function $g(\theta)$ at x = 0.0, 0.10, 0.25, 0.40, 0.5, 0.60, 0.75, 0.90, and 1.0.

From Fig. 6, we found that all the partial bond-angle distribution functions $g_{\alpha\beta\gamma}(\theta)$ have their peaks centered around the tetrahedral angle ($\theta = 109.47°$). But both the magnitude and the position of the peaks change as the composition changes and hence so do their contributions to the total bond-angle distribution function $g(\theta)$. For example, $g_{SiSiSi}(\theta)$ contributes the most to the total bond-angle distribution function $g(\theta)$ in the case of $x = 0.25$. The magnitude of its peak shows a monotonical decrease as x increases towards the Ge-rich region. Simultaneously, the position of its peak shifts from $\theta = 109.7°$ at $x = 0.25$ to $\theta = 110.1°$ at x = 0.75. On the other hand, the magnitude of the peak of $g_{GeGeGe}(\theta)$ decreases monotonically as x decreases towards the Si-rich region while the position of the peak shifts from

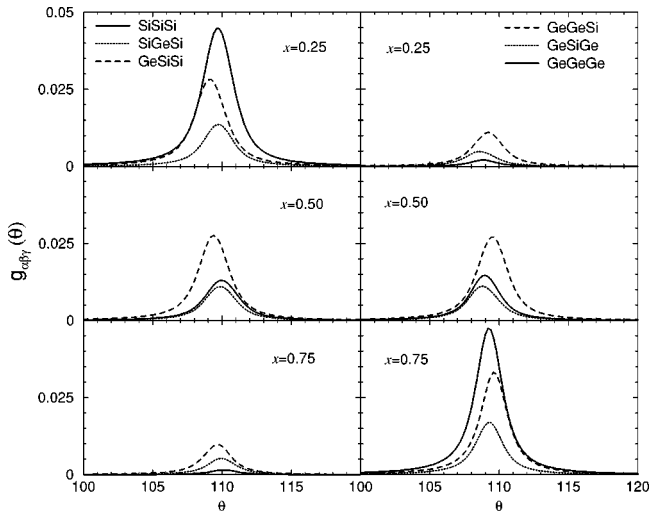FIG. 6. The partial bond-angle distribution function $g_{\alpha\beta\gamma}(\theta)$ at x = 0.25, 0.5, and 0.75. The left panel shows the results corresponding to $g_{SiSiSi}(\theta)$ (solid line), $g_{SiGeSi}(\theta)$ (dotted line), and $g_{GeSiSi}(\theta)$ (dashed line). The right panel shows the results corresponding to $g_{GeGeGe}(\theta)$ (solid line), $g_{GeSiGe}(\theta)$ (dotted line), and $g_{GeGeSi}(\theta)$ (dashed line).
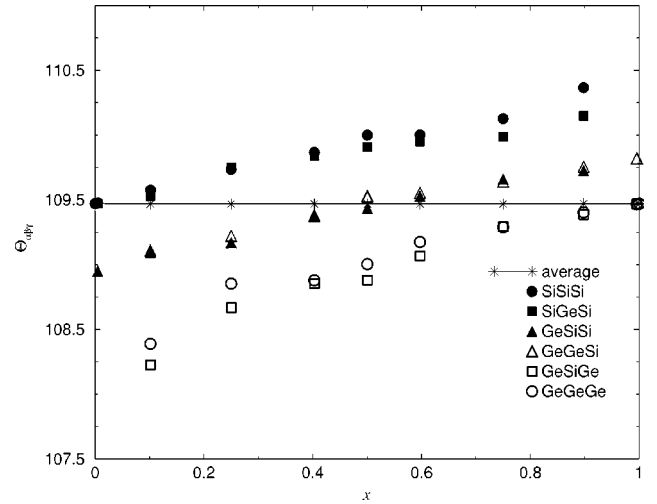

FIG. 7. The average bond angle $\bar{\Theta}_{\alpha\beta\gamma}$ as a function of the composition x. Note that the stars denote the overall average bond angle, the solid (open) circles $\bar{\Theta}_{SiSiSi}(\bar{\Theta}_{GeGeGe})$, the solid (open) squares $\bar{\Theta}_{SiGeSi}$ ($\bar{\Theta}_{GeSiGe}$), and the solid (open) up-triangles $\bar{\Theta}_{GeSiSi}$ ($\bar{\Theta}_{GeGeSi}$), respectively. The solid line denotes the tetrahedral angle of 109.47°.

$\theta = 109.3°$ at $x = 0.75$ to $\theta = 108.8°$ at $x = 0.25$. In the vicinity of $x = 0.5$, however, all of the partial bond-angle distribution functions $g_{\alpha\beta\gamma}(\theta)$ contribute to the total bond-angle distribution function $g(\theta)$ with comparable weights.

An interesting feature is that the average bond-angles always keep in the order of $\bar{\Theta}_{SiSiSi} > \bar{\Theta}_{SiGeSi} > \bar{\Theta}_{GeSiSi} > \bar{\Theta}_{GeSiSi} > \bar{\Theta}_{GeGeGe} > \bar{\Theta}_{GeSiGe}$, independent of the composition (see Fig. 7). In particular, it is found that the deviations of $\bar{\Theta}_{SiSiSi}$ (solid circles) and $\bar{\Theta}_{SiGeSi}$ (solid squares) from the tetrahedral angle are always positive while those of $\bar{\Theta}_{GeGeGe}$ (open circles) and $\bar{\Theta}_{GeSiGe}$ (open squares) always negative. This can be understood as follows. The average bond-angle $\bar{\Theta}_{SiSiSi}$ ($\bar{\Theta}_{SiGeSi}$) between two Si-Si bonds (two Ge-Si bonds) depends on how the lattice constant of the $Si_{1-x}Ge_x$ alloys at a certain composition x compares with that of bulk Si. Since the lattice constant of the alloy is always greater than that of the bulk Si and it increases with increasing x, the average bond angle $\bar{\Theta}_{SiSiSi}$ ($\bar{\Theta}_{SiGeSi}$) will therefore always be greater than the overall average bond-angle (almost identical to the tetrahedral angle of 109.47°) and increases with increasing x (see Fig. 7). Hence, a positive angular deviation of $\bar{\Theta}_{SiSiSi}$ ($\bar{\Theta}_{SiGeSi}$) from the overall average bond-angle results and this angular deviation increases with increasing x (towards the Ge-rich region). By the same token, since the lattice constant of the alloy is always less than that of bulk Ge, the average bond-angle $\bar{\Theta}_{GeGeGe}$ ($\bar{\Theta}_{GeSiGe}$) will always be less than the overall average bond angle and decreases with decreasing x. Thus, a negative angular deviation from the average bond-angle results for the average bond-angle $\bar{\Theta}_{GeGeGe}$ ($\bar{\Theta}_{GeSiGe}$) and this negative deviation decreases with decreasing x (towards the Si-rich region). This scenario also indicates that the largest positive angular deviation for

TABLE I. The local electron distributions [the on-site orbital (s,p_x,p_y,p_z) electrons, the bond electrons associated with the atom at a given site with its nearest neighbors, and the total electrons associated with the atom at a given site] of the alloy $Si_{1-x}Ge_x$ with $x \approx 0.1$ (194 Si atoms and 22 Ge atoms in the supercell). The first column gives the atomic site label which indicates the position of the atom in the supercell (see details in Sec. IV). Note that the result is obtained in the framework of sp^3 basis set.

Site label	s	p_x	p_y	p_z	Bond electrons	Total electrons
1 (Ge)	1.36413	0.50554	0.50491	0.50517	1.18629	4.06604
5 (Si)	1.23439	0.50791	0.50881	0.50834	1.22400	3.98344
70 (Si)	1.23474	0.50842	0.50851	0.50847	1.22387	3.98401
167 (Si)	1.23282	0.50800	0.50844	0.50834	1.22485	3.98245
200 (Si)	1.23460	0.50819	0.50884	0.50902	1.22405	3.98470
209 (Si)	1.23520	0.51266	0.51200	0.51179	1.23056	4.00220
210 (Si)	1.23458	0.51178	0.51219	0.51240	1.23107	4.00202
211 (Si)	1.23539	0.51216	0.51181	0.51152	1.23084	4.00171
212 (Si)	1.23517	0.51218	0.51267	0.51212	1.23047	4.00261
213 (Si)	1.23523	0.51142	0.51086	0.51186	1.22959	3.99896

$\bar{\Theta}_{SiSiSi}$ and $\bar{\Theta}_{SiGeSi}$ (of the order of $1°$) occurs in the Ge-rich region (large x) while the largest negative angular deviation for $\bar{\Theta}_{GeGeGe}$ and $\bar{\Theta}_{GeSiGe}$ ($\sim 1°$) occurs in the Si-rich region (small x). But, because the partial bond-angle distribution function $g_{SiSiSi}(\theta)$ [$g_{SiGeSi}(\theta)$] is insignificant in the Ge-rich region and $g_{GeGeGe}(\theta)$ [$g_{GeSiGe}(\theta)$] is insignificant in the Si-rich region, the large positive angular deviation of $\bar{\Theta}_{SiSiSi}$ ($\bar{\Theta}_{SiGeSi}$) and the large negative angular deviation of $\bar{\Theta}_{GeGeGe}$ ($\bar{\Theta}_{GeSiGe}$) will not manifest themselves in any significant way in the release of strain. However, in the neighborhood of $x=0.5$, both the positive angular deviation of $\bar{\Theta}_{SiSiSi}$ ($\bar{\Theta}_{SiGeSi}$) and the negative angular deviation of $\bar{\Theta}_{GeGeGe}$ ($\bar{\Theta}_{GeSiGe}$) are still substantial ($\sim 0.5°$) while their respective partial bond-angle distribution functions all make significant contributions to the total bond-angle distribution.

A closer examination of Figs. 6 and 7 reveals that in the vicinity of $x=0.5$, the magnitudes of the negative angular deviations of $\bar{\Theta}_{GeGeGe}$ and $\bar{\Theta}_{GeSiGe}$ are greater than or comparable to the positive angular deviations of $\bar{\Theta}_{SiSiSi}$ and $\bar{\Theta}_{SiGeSi}$. Furthermore, the magnitudes of the peaks of the partial bond-angle distribution functions $g_{GeGeGe}(\theta)$ and $g_{GeSiGe}(\theta)$ are greater than those of $g_{SiSiSi}(\theta)$ and $g_{SiGeSi}(\theta)$. The combination of those effects leads to the situation where the negative angular deviations outweigh the positive angular deviations. A net negative angular deviation in the bond-angle manifests itself in the reduction of the lattice constant. Hence, in the vicinity of $x=0.5$, it is the bond angle relaxation that leads to the negative deviation from Vegard's law in the lattice constant.

Based on the local structural analysis, we have established how the local structure changes and how these changes are the result of the accommodation to the strain relaxation. Even though Si-Si, Si-Ge, and Ge-Ge pairs in the alloys prefer to maintain their respective bond lengths so that their respective bond lengths are, for the most part, insensitive to the change in the composition, the average overall bond length nevertheless shows a linear dependence on the composition. The strain relaxation can therefore be separated into

two parts: the radial relaxation and the angular relaxation. The former is responsible for the general trend of a linear dependence on the composition, and the latter is responsible for the negative deviation in the lattice constant in the vicinity of $x=0.5$.

IV. LOCAL ANALYSIS OF ELECTRONIC STRUCTURE

Having identified the mechanism for the strain release associated with the lattice mismatch and established the link between the local structural changes and the mechanisms for the strain release, it would be illuminating if one can gain an understanding of the interplay among the local electronic structure, local structural changes, and the strain-relaxation. For this purpose, we conducted a local analysis of the electronic structure for $Si_{1-x}Ge_x$ alloys, using the approach developed in Ref. 26. The analysis was carried out in the framework of the sp^3 basis set used in the "*ab initio*" molecular dynamics scheme. In Tables I and II, we list the local electron distributions (the on-site orbital electrons, the bond electrons, and the total site electrons) for two alloy configurations corresponding to $x \approx 0.1$ and $x \approx 0.9$, respectively. Specifically, for each of these configurations, we present the results for local electron distributions in two regions: (a) one in the vicinity of an impurity atom and (b) in the vicinity of a host atom (which is at least beyond the second nearest neighbors of the impurity atom). In Table I (corresponding to a Si-rich configuration with $x=0.1$), the local electron distributions in the region surrounding a Ge impurity at site 1 with 4 nearest neighbor Si atoms at sites 5, 70, 167, and 200, respectively and those in the region, away from the impurity at site 1, surrounding a host Si atom at site 213 with 4 nearest neighbor Si atoms at sites 209, 210, 211, and 212 are given. From Table I, it is seen that the charge transfer occurs between the Ge impurity atom and its 4 nearest neighbor Si atoms in the region surrounding the impurity while there is no significant charge transfer amongst the Si atom and its neighbors in the region away from the immediate neighborhood of the impurity. From the results shown in Tables I and II, it can be seen that the electron transfer always occurs

TABLE II. The local electron distribution [the on-site orbital (s, p_x, p_y, p_z) electrons, the bond electrons associated with the atom at a given site with its nearest neighbors, the total electrons associated with the atom at a given site] of the alloy $Si_{1-x}Ge_x$ with $x \approx 0.9$ (22 Si atoms and 194 Ge atoms in the supercell). The first column gives the site label which indicates the position of atom in the supercell (see details in Sec. IV). Note that the result is obtained in the framework of sp^3 basis set.

Site label	s	p_x	p_y	p_z	Bond electrons	Total electrons
25 (Ge)	1.37737	0.49334	0.49340	0.49316	1.15640	4.01367
26 (Ge)	1.37615	0.49374	0.49376	0.49358	1.15781	4.01504
27 (Ge)	1.37787	0.49430	0.49424	0.49440	1.15614	4.01695
28 (Ge)	1.37739	0.49370	0.49358	0.49447	1.15631	4.01544
29 (Si)	1.24569	0.49890	0.49896	0.49910	1.19274	3.93539
41 (Ge)	1.37833	0.49107	0.49134	0.49121	1.14972	4.00167
42 (Ge)	1.37836	0.49046	0.49051	0.49103	1.15002	4.00037
43 (Ge)	1.37892	0.49140	0.49139	0.49130	1.14951	4.00252
44 (Ge)	1.37801	0.49069	0.49059	0.49041	1.15051	4.00021
45 (Ge)	1.37814	0.49045	0.49013	0.49083	1.14994	3.99949

from the Si atom to the Ge atom as expected because of the higher electronegativity of the Ge atom with respect to the Si atom. For example, each of the 4 nearest neighbor Si atoms transfers about 0.017e to the impurity Ge atom at the center, leading to a gain of about 0.066e for the Ge impurity atom. The transfer of the electrons comes mostly from the Si p orbitals to Ge p orbitals, with the remainder contributing to the enhancement of the bond charge for the formation of Ge-Si bond, as can be seen from the results shown both in Table I ($x=0.1$, Si-rich configuration) and Table II ($x=0.9$, Ge-rich configuration). For the Ge-rich configuration, the charge transfers again are mainly concentrated in the immediate vicinity of the impurity (Si). For example, it can be seen from Table II that 0.065e are transferred from the impurity Si atom (at site 29) to its 4 nearest neighbor Ge atoms (at sites 25, 26, 27, and 28, respectively), each gaining on the average about 0.016e. In the region away from the immediate neighborhood of the impurity Si atom, there is hardly any charge transfer between the host Ge atom at site 45 (center) and its 4 nearest neighbor host Ge atoms (at sites 41, 42, 43, and 44, respectively). From Table I, one obtains the average bond charge for a pair of Si-Si bond to be about 0.62e. From Table II, one obtains the average bond charge for a pair of Ge-Ge bond to be about 0.58e. From Tables I and II, one obtains the average bond charge for a Si-Ge bond to be about 0.60e. Thus the sequence of average bond charges follows the order $\bar{q}_{bond}(Ge\text{-}Ge) < \bar{q}_{bond}(Si\text{-}Ge) < \bar{q}_{bond}(Si\text{-}Si)$, providing the electronic basis for the observation of average bond-lengths in the order of $b_{GeGe} > b_{SiGe} > b_{SiSi}$ (see Sec. III). Our local analysis also finds that the average bond charges for the Ge-Ge, Ge-Si, and Si-Si pairs show weak dependence on the composition. However, the overall average bond charge shows a general trend of linear dependence on the composition. These results provide the electronic basis for the relationships established for various average bond lengths in the structural analysis given in Sec. III.

V. CONCLUSION

In conclusion, our *ab initio* molecular dynamics study of $Si_{1-x}Ge_x$ alloys provide a comprehensive understanding of the interplay between the strain relaxation associated with the lattice mismatch and the changes in the local structural and electronic properties. We find that Si and Ge atoms do not have a strong preference to form either the Si-Si or the Ge-Ge pair but are fully miscible in the $Si_{1-x}Ge_x$ alloys because of the similar chemical properties. In the relaxation process, most of the Si-Si and Ge-Ge pairs try to maintain their equilibrium distances corresponding to their pure limits, leading to a weak dependence of the average bond length for Si-Si, Si-Ge, and Ge-Ge pairs on the composition. However, the overall average bond length does show a linear dependence on the composition (see Fig. 3), indicating that the radial relaxation is mainly responsible for the general trend of a linear dependence of the lattice constant on the composition. On the other hand, the bond-angle relaxation in the vicinity of $x=0.5$ has been shown to be responsible for the negative deviation of the lattice constant from the Vegard's law. Finally, we would like to remark that, unlike $Si_{1-x}Ge_x$ alloys which are fully miscible due to the similar chemical properties of Si and Ge, alloys of III-V compounds are usually immiscible at equilibrium.[27]

[1] L. Incocia, S. Mobilio, M. G. Proietti, P. Fiorini, C. Giovannella, and F. Evangelisti, Phys. Rev. B **31**, 1028 (1985); A. Filliponi, P. Fiorini, F. Evangelisti, A. Balerna, and S. Mobilio, J. Phys. (Paris), Colloq. **8**, 357 (1986).

[2] Y. Nishino, S. Muramatsu, Y. Takeno, and H. Kajiyama, Phys. Rev. B **38**, 1942 (1988).

[3] H. Kajiyama, S. Muramatsu, T. Shimada, and Y. Nishino, Phys. Rev. B **45**, 14 005 (1992).

[4] M. Matsuura, J. M. Tonnerre, and G. S. Cargill, Phys. Rev. B **44**, 3842 (1991).

[5] J. C. Woicik, C. E. Bouldin, M. I. Bell, J. O. Cross, D. J. Tweet, B. D. Swanson, T. M. Zhang, L. B. Sorenson, C. A. King, J. L. Hoyt, P. Pianetta, and J. F. Gibbons, Phys. Rev. B **43**, 2419 (1991); J. C. Woicik and C. E. Bouldin, *ibid.* **55**, 15 386 (1997); J. C. Woicik, K. E. Miyano, C. A. King, R. W. Johnson, J. G. Pellegrino, T.-L. Lee, and Z. H. Lu, *ibid.* **57**, 14 592 (1998).

[6] D. B. Aldrich, R. J. Nemanich, and D. E. Sayers, Phys. Rev. B **50**, 15 026 (1994).

[7] S. Wei, H. Oyanagi, H. Kawanami, K. Sakamoto, T. Sakamoto, K. Tamura, N. L. Saini, and K. Uosaki, J. Appl. Phys. **82**, 4810 (1997).

[8] A. P. Hitchcock, T. Tyliszczak, P. Aebi, J. Z. Xiong, T. K. Sham, K. M. Baines, K. A. Muller, X. H. Feng, J. M. Chen, B. X. Yang, Z. H. Lu, J.-M. Baribeau, and T. E. Jackman, Surf. Sci. **291**, 349 (1993); A. P. Hitchcock, T. Tyliszczak, P. Aebi, X. H. Feng, Z. H. Lu, J.-M. Baribeau, and T. E. Jackman, *ibid.* **301**, 260 (1994); T. Tyliszczak, A. P. Hitchcock, Z. H. Lu, J.-M. Baribeau, and T. E. Jackman, Scanning Microsc. **8**, 795 (1994).

[9] J. C. Aubry, T. Tyliszczak, A. P. Hitchcock, J.-M. Baribeau, and T. E. Jackman, Phys. Rev. B **59**, 12 872 (1999).

[10] R. W. Olesinski and G. J. Abbaschian, Bull. Alloy Phase Diagrams **5**, 180 (1984).

[11] J. P. Dismukes, L. Ekstrom, and R. J. Paff, J. Phys. Chem. **68**, 3021 (1964).

[12] J. L. Martins and A. Zunger, Phys. Rev. B **30**, 6217 (1984); Phys. Rev. Lett. **56**, 1400 (1986).

[13] M. R. Weidmann and K. E. Newmann, Phys. Rev. B **45**, 8388 (1992).

[14] M. Ichimura, Y. Nishino, H. Kajiyama, and T. Wada, Jpn. J. Appl. Phys., Part 1 **29**, 842 (1990).

[15] S. de Gironcoli, P. Giannozzi, and S. Baroni, Phys. Rev. Lett. **66**, 2116 (1991).

[16] A. Qteish and R. Resta, Phys. Rev. B **37**, 1308 (1988).

[17] Y. Cai and M. F. Thorpe, Phys. Rev. B **46**, 15 872 (1992); **46**, 15 879 (1992); N. Mousseau and M. F. Thorpe, *ibid.* **48**, 5172 (1993).

[18] N. Mousseau and M. F. Thorpe, Phys. Rev. B **46**, 15 887 (1992).

[19] B. Dünweg and D. P. Landau, Phys. Rev. B **48**, 14 182 (1993).

[20] L. Vegard, Z. Phys. **5**, 17 (1921).

[21] L. Pauling, *The Nature of the Chemical Bond* (Cornell University Press, Ithaca, NY, 1967).

[22] S. G. Shen, D. X. Zhang, and X. Q. Fan, J. Phys.: Condens. Matter **7**, 3529 (1995).

[23] O. F. Sankey and D. J. Niklewski, Phys. Rev. B **40**, 3979 (1989); A. A. Demkov, J. Ortega, O. F. Sankey, and M. P. Grumbach, *ibid.* **52**, 1618 (1995).

[24] D. R. Hamann, M. Schlüter, and C. Chiang, Phys. Rev. Lett. **43**, 1494 (1979).

[25] D. M. Ceperley and G. J. Alder, Phys. Rev. Lett. **45**, 566 (1980); J. Perdew and A. Zunger, Phys. Rev. B **23**, 5048 (1981).

[26] D. R. Alfonso, S. Y. Wu, C. S. Jayanthi, and E. Kaxiras, Phys. Rev. B **59**, 7745 (1999).

[27] D. W. Jenkins, K. E. Newmann, and J. D. Dow, Phys. Rev. B **32**, 4034 (1985).